Embedded-based Wireless Pressure Signal Waveform Display

Lv Yalei, Ma Xin

Abstract—**This paper presents a wireless pressure signal real-time acquisition and waveform display system based on embedded technology. The system takes the STM32F103RCT6 microcontroller as the core, and combines the high-precision ADC analog-to-digital conversion module, LCD display module and serial communication module to realize the digital acquisition, processing and visualization of pressure signals. Through the synchronous working mode of ADC+DMA+TIMER, the system can dynamically adjust the sampling frequency and store the data in real time, and use the FFT algorithm to complete the frequency domain analysis, and at the same time, realize the parameter adjustment through external interrupt. The experimental results show that the system can accurately collect the pressure signal and display the waveform in real time through the LCD screen, and the serial communication function supports the data analysis of the host computer. The test data show that the average value of sensor output voltage is negatively correlated with the pressure in the pressure range of 50g to 200g weights (R²>0.98), which verifies the reliability and accuracy of the system. The design provides an efficient solution for monitoring pressure signals in industrial monitoring, medical equipment and other fields.**

Index Terms—**Embedded system; FFT analysis; Pressure sensor; Waveform display; Wireless transmission**

I. INTRODUCTION

In today's era of rapid development of intelligence and automation, embedded systems play a key role in many fields by virtue of their efficient performance, flexible customization and optimal management of resources. From industrial automation control[1][2] to intelligent medical devices[3][4] to Internet of Things applications[5], embedded systems have become one of the core technologies to realize equipment intelligence and function integration.

Pressure sensors, as a key sensing element capable of converting pressure signals into electrical or other measurable signals, have an equally wide range of applications. In the aerospace field, pressure sensors are used to monitor changes in air pressure and structural stress in aircraft[6][7]; in the automotive industry, they are used for tire pressure monitoring, oil pressure detection and other key aspects[8][9].

Previous research works have explored various aspects of the integration of embedded systems with pressure sensors.Popal et al[10] proposed a pressure sensor data acquisition and processing system based on an embedded

  Lv Yalei, School of Computer Science and Technology, Tiangong University, Tianjin, China
  Ma Xin, School of Computer Science and Technology, Tiangong University, Tianjin, China

microcontroller, which is able to collect the signals from the pressure sensor in real time and accurately, and analyze and process the data through algorithms to effectively improve the accuracy and reliability of pressure monitoring. While Basu[11] explored how to optimize the energy management of pressure sensors on a low-power embedded platform to extend the device's endurance.

Emilio[12] focused on how to improve the accuracy of pressure sensor signal acquisition. By optimizing the hardware circuit design and software algorithms of the embedded system, the noise interference in the signal acquisition process was reduced, and the high-precision acquisition of the pressure signal was achieved, which provided a reliable data basis for the subsequent pressure data analysis and application.

Compared with traditional pressure monitoring and processing methods, the combination of embedded and pressure sensors shows many significant advantages. In the traditional mode, the collection of pressure data often relies on independent sensor devices, which are relatively single-function, lack of effective data processing and analysis capabilities, and need to manually carry out a large number of data recording and post-processing, which is inefficient and prone to errors. The combination of embedded systems and pressure sensors builds a highly integrated intelligent system. The powerful computing and control capabilities of the embedded system can quickly analyze and process a large amount of data collected by the pressure sensor in real time without too much manual intervention, greatly improving the efficiency and accuracy of data processing[13].

This study develops a wireless pressure signal real-time acquisition and processing system based on embedded technology, which successfully realizes the pressure-electric signal conversion and waveform visualization monitoring. The system adopts high-precision AD conversion module to digitize the sensor signals, and realizes the real-time display of pressure waveform through LCD display. On this basis, the integrated serial communication module realizes data transmission and supports the analysis and display of voltage signals on the PC, which provides a new solution for the intelligent upgrade of the pressure monitoring system.

II. METHODS

A. Embedded System Design Ideas

In this study, the input analog signal is captured through the ADC analog-to-digital converter module; the sampling is triggered once by the PWM output of the timer, so the sampling frequency can be set by the timer. Then the data sampled by the ADC is sent to the specified memory by

means of DMA. At the same time, the sampled data will be compared by loop to get the maximum and minimum values, and the signal amplitude will be obtained by subtracting the two. The sampled data is then transformed by FFT, and the frequency of the signal is obtained after a series of calculations. The obtained signal calculation content is sent to the PC through UART1, and the baud rate can be set. The setting of the sampling rate and the design of the serial output are carried out through external interrupts. This experiment indicates whether the system is working or not through LEDs. At the same time, the waveform of the input signal and the calculation results are displayed on the LCD screen, and the LCD display uses the LCD driver function provided by Positive Point Atom.
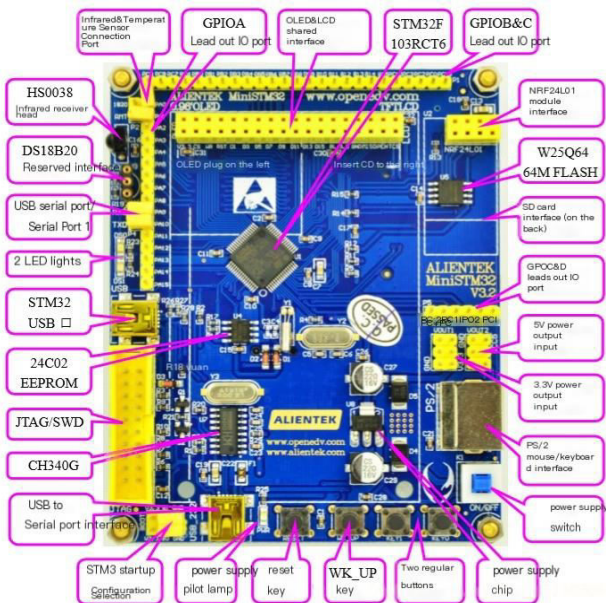
Fig.1.Introduction to the development board modules

B. Hardware Design

1) STM32 minimum system design

The core processor of this system adopts the STM32F103RCT6 microcontroller with ARM Cortex-M3 architecture, which contains the following hardware features: 256KB Flash program memory and 48KB SRAM data storage area are integrated inside the chip; multiple types of timer modules are integrated (2 basic, 4 general-purpose, and 2 advanced timers); rich peripheral interface Resources (including 3 SPI, 2 IIC, 5 UART, USB2.0 full-speed interface and CAN bus controller); configured with 12-channel DMA transfer module and 51 programmable GPIO ports. The clock system uses an external 8MHz quartz crystal oscillator as the base frequency source, through the integrated phase-locked loop (PLL) module to implement the frequency multiplication process, and ultimately increase the system's operating frequency to 72MHz. in terms of power management, the main control chip adopts a 3.3V DC power supply scheme, which is connected to the digital-to-analog conversion module with an external 5V reference voltage source. The analog signal processing unit contains three 12-bit precision ADC sampling channels and one 12-bit DAC output channel. The hardware reset circuit is connected to the NRST pin and supports manual reset function. The system

also integrates SDIO memory expansion interface to provide convenience for peripheral device expansion. The download circuit adopts JTAG download.

The internal resources used in this design are SRAM, FLASH, General Purpose Timer 2, DMA1, UART1, DAC1, GPIOA, EXTI.
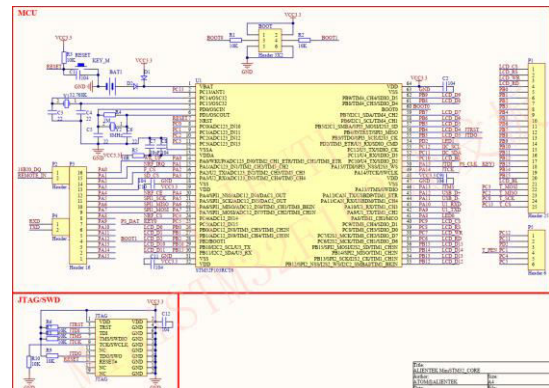
Fig.2.STM32F103RCT6 minimum system circuit diagram

2) LED display and external interrupt key circuitry

The LED driver circuit adopts the anode connected to the power supply program, the protection resistor is connected in series to the power supply circuit, and the cathode of the light-emitting diode is directly connected to GPIOA_Pin_8. The IO port is configured as a push-pull output mode, which forms a cutoff loop when the port outputs a high potential to turn off the light, and conducts when the output is low. The key connection circuit is shown in Figure 3. WK_UP key is connected to PA0 pin, which triggers the rising edge interrupt event of EXTI0; KEY0 and KEY1 are connected to PC5 and PA15 pins respectively, which correspond to the two interrupt channels of EXTI5 and EXTI15, and they are all set to falling edge trigger mode. Among them, PA15 should pay attention to the configuration of the multiplexing function, and the default debug port multiplexing state needs to be lifted for normal use.

Fig.3.LED and key circuit

3) LCD display interface circuit

A 2.8-inch TFT-LCD display module was selected for this design, and its hardware parameters include a 320 × 240 pixel resolution and 65536 color display capability. The module is configured with a 16-bit parallel interface (80 parallel port) and integrated touch function, and the circuit connection is realized through 2 × 17 specification 2.54mm pitch male pins. The display driver core adopts ILITEK's ILI9341 controller, which has a built-in graphics cache unit and can flexibly set the display area and color parameters through register commands to realize multi-window graphics rendering.Supporting development platform has integrated standard display module interface, the user only through the row of pins directly connected to complete the hardware docking, the interface circuit shown in Figure 4:
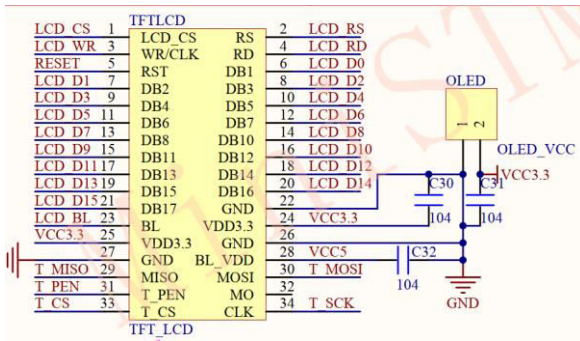
Fig.4.TFT_LCD interface circuit

C. System programming

1) Overall flow of program design

The main function execution process of the embedded system designed in this study is shown in Fig. 5.
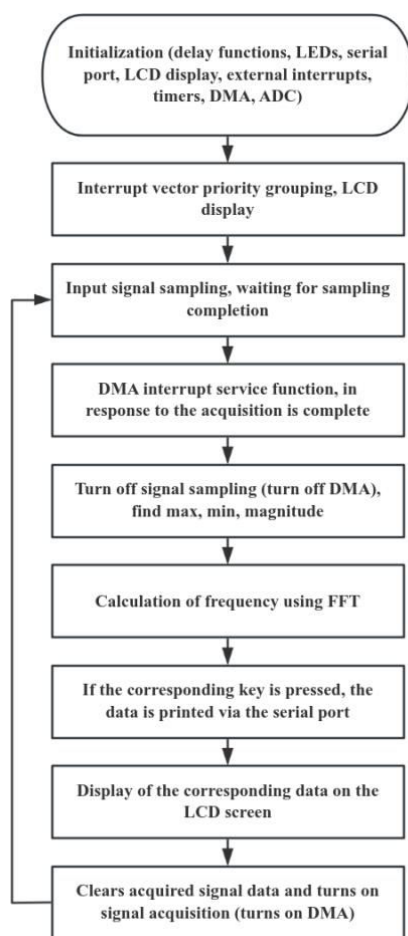
Fig.5.Main function execution flow

Sampling parameters can be adjusted according to the key operation: triggering KW_UP will enhance the timer crossover coefficient, realizing the attenuation response of the sampling frequency;operating KEY1 adjusts the crossover parameter in reverse, enhancing the system sampling rate; activating KEY0 will start the serial communication module, performing the uploading task of the terminal data. Signal acquisition adopts ADC+DMA+TIMER, the acquisition is completed, DMA interrupt is triggered, and the acquisition is completed to mark the position bit.

2) Key interrupt program design

The three keys KEY_UP, KEY1 and KEY2 are connected to the PA0, PC5 & PA15 ports respectively. The PA0 pin is set to pull-down input operation mode, while the PC5 and PA15 pins are configured with pull-up input. The interrupt triggering condition is set as follows: PA0 detects the rising edge signal and PC5 and PA15 detect the falling edge signal. Before initializing the GPIO, make sure that the corresponding peripheral clock has been enabled through the RCC register.

The corresponding interrupt channels for PA0, PC5, and PA15 are channels 0, 5, and 15. The external interrupts configure the mode of the response and enable it, and then configure the NVIC of the response and enable the NVIC, and their corresponding preemptive priorities are all 2, and their sub-priorities are 0, 1, and 2.

In the respective interrupt service function, it first determines whether the corresponding key is pressed or not, and if it is pressed, it performs the corresponding function and then clears the corresponding external interrupt.

3) Data Acquisition Module Programming

The data acquisition module mainly consists of TIMER, DMA and ADC1. In this experiment, the PA1 port is used as the data acquisition port, and Timer 2 is configured as PWM mode. The sampling rate of the analog-to-digital converter can be dynamically adjusted by adjusting the frequency parameter of the pulse width modulation signal. The system uses a direct memory access channel (DMA1) to realize the automatic handling of the acquired data, and stores the conversion results in real time to the designated memory area to ensure the high efficiency of the data transfer process to support the subsequent digital signal processing work.

The clock source of GPIOA and ADC1 should be turned on first, followed by configuring the PA1 pin to analog input mode. ADC1 selects channel 1 to use regular conversion, configured to continuous conversion mode, the trigger mode selects T2_CC2, i.e., timer 2, the data is selected to be right-aligned,and the number of channels for regular-sequence conversion is 1, and the sampling time is set to cycles.

After ADC1 is set up, enable ADC1 and reset the calibration register of the specified ADC for calibration.

Then the clock of the timer is enabled, and the prescaler value and count value of counter 2 are passed in through an external parameter, which can be set so that the sampling frequency can be adjusted. The counter is set to count up mode. The output is set to PWM1 with output polarity low and TIM_Pulse is set to set the duty cycle. Finally TIM2 is enabled.

Finally enable channel 1 of DMA1, first turn on the clock of DMA1, transfer the data from ADC1 into memory, set the amount of data transferred at one time to 1024 bytes, the number of data bits of both memory and peripheral devices is 16 bits, and the cyclic transfer, the priority is set to the highest. Turn on the interrupt of DMA1, respond to the interrupt when one DMA transfer is completed, notify the completion of one data sampling in the interrupt service function, and set both the preemption priority and the sub-priority to 0.

4) Serial Programming

In this experiment, the corresponding data is transmitted to

the host computer through UART1, and the corresponding ports of UART1 are PA9 and PA10. The configuration flow of UART1 peripheral is as follows: firstly, it is necessary to activate the clock source of the relevant modules, including the GPIOA port and the UART1 bus. For the pin function assignment, PA9 should be configured as a push-pull output structure in the multiplexing mode, and PA10 should be set as a floating input state to adapt to the receiving function. The communication parameter setting link needs to specify the transmission format: define the data frame as 8-bit effective length, single stop bit structure, disable the parity function, and disable the hardware flow control mechanism.

In the development of embedded systems, if you need to redirect the printf function to the serial communications interface, can be realized through the following steps: first of all, in the project code to add a specific implementation of the fputc (int ch, FILE * f) function, and contains the standard input and output header file ＂stdio.h＂. Through this configuration, the system is able to transmit the output data of the printf function through the serial port.

5) FFT Calculation Frequency

In the field of signal analysis, Fourier transform, as one of the key techniques, can transform the time-dimensioned signals into frequency-domain expressions, and then analyze the frequency composition of the signals. The traditional Discrete Fourier Transform (DFT) uses direct computation, so its time complexity is high and it is seldom used in scenarios with strict real-time requirements. The Fast Fourier Transform (FFT) algorithm optimizes the computational process by tapping into the symmetry and periodicity characteristics of the signal, significantly reducing the amount of computation. This improvement makes the frequency domain analysis method more widely used in many fields such as communication systems, biomedical engineering, etc., and promotes the development process of related technologies.

As the theoretical basis of Fast Fourier Transform (FFT), Discrete Fourier Transform (DFT) is the core algorithm to realize spectrum analysis in the field of digital signal processing. This mathematical method constructs a two-way conversion bridge between the time domain and the frequency domain by discretizing the sampled data. For a discrete time series $x(n)$ of length N, its discrete Fourier transform is defined as:

$$X(k) = \sum_{n=0}^{N-1} x(n)e^{-j\frac{2\pi}{N}kn}, k = 0,1,\cdots,N-1 \qquad (1)$$

In terms of computational complexity, direct computation of DFT requires N^2 complex multiplications and $N(N-1)$ complex additions, which is huge when N is large, limiting its application in practice.

The core principle of Fast Fourier Transform (FFT) lies in the use of partitioning strategy to transform high-dimensional signal processing into low-dimensional computation. By exploiting the symmetry and periodicity of the complex exponential function, the algorithm effectively reduces the dimensionality of the traditional DFT and significantly improves the computational efficiency. In specific implementation, the algorithm transforms the original signal sequence into multiple sub-sequences in parallel through recursive decomposition technique, thus reaching a significant optimization of complexity scale.

Taking the base-2 time extraction (DIT) FFT algorithm as an example, the basic steps are as follows:

Sequence grouping:A sequence $x(n)$ of length N ($N = 2^M$, M is a positive integer) is divided into a sequence of odd terms $x_1(r)$ and a sequence of even terms $x_2(r)$ in chronological order, where $r = 0,1,\cdots,\frac{N}{2} - 1$, $x_1(r) = x(2r)$, $x_2(r) = x(2r + 1)$.

Recursive computation: the DFT of the original sequence can be expressed as:

$$X(k) = X_1(k) + W_N^k X_2(k), \quad k = 0,1,\cdots,\frac{N}{2} - 1 \qquad (2)$$

$$X\left(k + \frac{N}{2}\right) = X_1(k) - W_N^k X_2(k), \quad k = 0,1,\cdots,\frac{N}{2} - 1 \qquad (3)$$

where $W_N^k = e^{-j\frac{2\pi}{N}k}$ is the rotation factor.

Repeat decomposition: continue similar decomposition for $X_1(k)$ and $X_2(k)$ until the decomposition is a sequence of length 1.

In this way, the computational complexity of the base-2 time extraction FFT algorithm is reduced to $O(N\log_2 N)$ complex multiplications and $O(N\log_2 N)$ complex additions, which greatly improves the computational efficiency compared with the direct computation of DFT.

In this experiment, 1024 consecutive sampling points are analyzed for spectrum analysis, and the Fast Fourier Transform is completed by calling the FFT library function. Peak detection is performed on the spectral data after processing to obtain the frequency component with the largest energy. According to the Nyquist-Shannon sampling theorem, in order to ensure the accurate reconstruction of the original signal spectrum, the sampling frequency of the system needs to meet the condition of fs>2fmax, where fmax is the highest frequency component of the signal. The main frequency characteristics of the signal can be effectively extracted by the above method. The frequency of the sampled signal is fus=72000000/(T*psc), where T is the count value of the STM32 timer and psc is the crossover frequency value. $X_a(k * F) = T * X(k) = T * DFT[x(n)]_N$, where

$$F = \frac{1}{Tp} = \frac{1}{NT} = \frac{fus}{N} \qquad (4)$$

X_a is the spectral function of the analog signal, $X(k)$ is the discrete Fourier transform of the sampled signal, and F denotes the sampling interval of the spectrum of the analog signal, which is called the frequency resolution. So if the maximum frequency is achieved when k=temp, then the maximum frequency is f=temp*F=temp*fus/n, (n is the number of points sampled at one time). cr4_fft_1024_stm32(fftout,fftin,n) is the library function used in the program to perform the FFT transform, fftin is the array of input signals captured. fftout is the array of outputs, and n is the number of points. fftout has 32 bits for each point, with the high 16 bits being the real part of the FFT transform and the low 16 bits being the imaginary part. The fftout is transformed and then k is found when the frequency amplitude is maximized, i.e., the maximum frequency is found.

6) LCD display interface program design

This design uses 2.8-inch TFT-LCD display screen, and its supporting library functions to complete the system development. First call "LCD_Init ()" function for initialization. Subsequently call windows () function to generate the basic display interface. After sampling 1024 points, the corresponding points will be displayed on the LCD screen, that is, the formation of waveforms.

III. EXPERIMENTS AND RESULTS

A. Experimental environment

The overall experimental environment of the embedded system is shown in Fig. 6, which mainly includes: 12V DC output power supply, transmitting module and piezoresistive flexible pressure sensor, receiving module, transparent acrylic plate, weights, STM32Mini development board, and the upper PC used for serial communication, where the power supply is mainly used to supply power to the transmitting end to generate an alternating magnetic field; the flexible pressure sensor and the transmitter and receiver modules are used to realize wireless transmission of pressure signals; the transparent acrylic plate is used to separate the double coils; the weights are used to simulate the external force applied to the flexible pressure sensor; the STM32Mini development board is used to process the pressure signals and display them; and the host PC is used to communicate with the STM32 through the serial port.
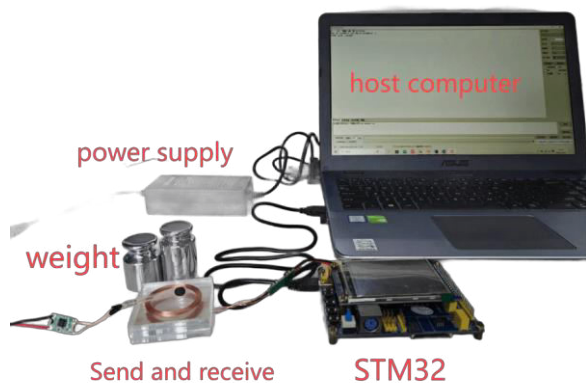
Fig.6.Embedded system stress test experimental environment construction

B. Experimental results and analysis

Respectively, 50g, 100g, 150g, 200g weights experiment to take the results of three experiments, the results of the serial data obtained as shown in Figure 7

Fig.7 Serial port data

Fig.8 Development board waveform display

Considering that the sensitive area of the flexible pressure sensor does not exactly coincide with the bottom surface of the weights, the pressure equation can be passed

$$p = \frac{F}{S} \qquad (5)$$

The mass of the weights is changed into the pressure to be analyzed. According to the pressure formula 50g weights act on the flexible pressure sensor used in this study the pressure is about 6.242 Kpa. Similarly, the pressure of other weights of different masses can be obtained as shown in Table 1.

Table 1 Embedded system stress experiment results

P(KPa)	Vmax（mv)			Vaverage (mv)
6.242	3276	3251	3236	3254
12.484	3156	3161	3168	3162
18.726	3072	3072	3074	3073
24.968	2924	2922	2934	2927

In order to visualize the relationship between pressure and voltage, the experimental data were plotted as a line graph, as shown in Figure 9.
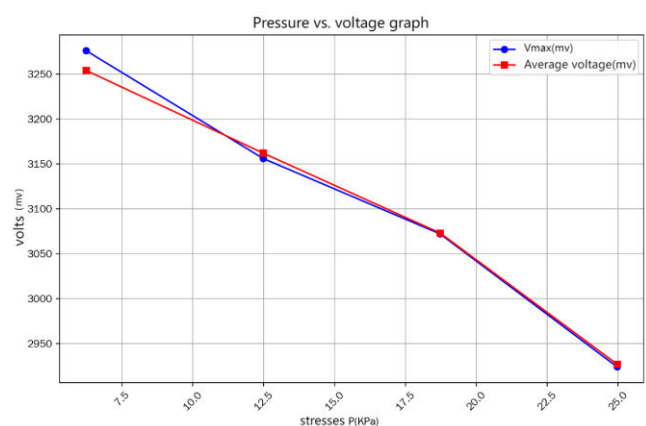
Fig.9.Line graph of pressure vs. voltage rms

The experimental results show that the mean value of the sensor output voltage is negatively correlated with the external pressure. As shown in Figs. 6-10, when the pressure increases from 6.242 kPa (50 g weight) to 24.968 kPa (200 g weight), the average value of the voltage decreases from 3254 mV to 2927 mV, which is a decrease of 10.05%. This phenomenon can be attributed to the fact that the resistance value of the flexible pressure sensor decreases with increasing pressure, leading to a decrease in the equivalent

impedance of the transmitting circuit, which in turn weakens the magnetic field coupling strength of the transmitting coil, and ultimately is reflected in the attenuation of the voltage amplitude at the receiving end.

REFERENCES

[1] Shylla, Dapynhunlang, et al. "Embedded systems in industrial automation 4.0." 2023 14th International Conference on Computing Communication and Networking Technologies (ICCCNT). IEEE, 2023.

[2] Minchala L I, Peralta J, Mata-Quevedo P, et al. An approach to industrial automation based on low-cost embedded platforms and open software[J]. Applied Sciences, 2020, 10(14): 4696.

[3] Garcia, A. Mendoza, et al. "Embedded platform for automation of medical devices." 2011 Computing in Cardiology. IEEE, 2011.

[4] Arandia N, Garate J I, Mabe J. Medical devices with embedded sensor systems: design and development methodology for start-ups[J]. Sensors, 2023, 23(5): 2578.

[5] Moreno, José David Alvarado, et al. "Embedded systems for internet of things (IoT) applications: a review study." 2018 Congreso Internacional de Innovación y Tendencias en Ingeniería (CONIITI). IEEE, 2018.

[6] Javed Y, Mansoor M, Shah I A. A review of principles of MEMS pressure sensing with its aerospace applications[J]. Sensor Review, 2019, 39(5): 652-664.

[7] Beutel T, Leester-Schädel M, Wierach P, et al. Novel pressure sensor for aerospace purposes[J]. IFSA Sens Transducers J, 2010, 115: 11-19.

[8] Soy H, Toy İ. Design and implementation of smart pressure sensor for automotive applications[J]. Measurement, 2021, 176: 109184.

[9] Tudor M J, Beeby S P. Automotive pressure sensors[M]. Momentum Press: New York, NY, USA, 2009.

[10] Popal M, Marcu M, Popa A S. A microcontroller based data acquisition system with USB interface[C]//International Conference on Electrical, Electronic and Computer Engineering, 2004. ICEEC'04. IEEE, 2004: 206-209.

[11] Basu S S. Hardware/software co-design and reliability analysis of ultra-low power biomedical devices[D]. EPFL, 2019.

[12] Emilio M D P. Embedded systems design for high-speed data acquisition and control[M]. Springer International Publishing, 2015.

[13] Kciuk M, Kowalik Z, Lo Sciuto G, et al. Intelligent medical velostat pressure sensor mat based on artificial neural network and arduino embedded system[J]. Applied System Innovation, 2023, 6(5): 84.

Lv Yalei graduate student, research direction: Flexible Pressure Sensors, Embedded System

Ma Xin graduate tutor, Ph.D. in Engineering, research direction: (1) Microfluidic biochip detection technology (2) Embedded system medical device design (3) Artificial intelligence drug design/screening, cell image analysis (4) Organoid chip bionics Model. He hosted and participated in 7 national, provincial, and ministerial level fund projects, and published more than ten academic papers as the first author.